This article has been accepted for publication in IEEE Photonics Journal. This is the author's version which has not been fully edited and content may change prior to final publication. Citation information: DOI 10.1109/JPHOT.2024.3386111

Fabrication of High Efficiency Green InGaN/GaN MicroLEDs by Modulating Potential Barrier Height of The Sidewall MQWs in V-pits

Hsin-Yu Liu, Donghao Zhang, Zhongying Zhang, Chaohsu Lai, Zongmin Lin, Chia-En Lee, Lijun Bao, Sheng-Po Chang *Member, IEEE,* and Shoou-Jinn Chang *Fellow, IEEE*

***Abstract*—In this study, Green MicroLEDs with different H_2 flow during the barrier growth are investigated. We observe that the Indium composition near V-pits affects potential barrier height of the sidewall multiple quantum wells (MQWs) thus has strong impact on screening effect of V-pits. EQE and relative IQE has a dramatically increase with more hydrogen flow during barrier growth, and thermal endurance and wavelength stability was also improved. The enhancement has been confirmed to come from the reduction of non-radiative recombination centers from small V-pits and higher potential barrier height on sidewall MQWs in V-shaped pits which screen dislocations (TDs). These results demonstrate the advantages of modification H_2 flow during barrier growth and also provide a new concept to modulate potential barrier height of the sidewall MQWs for better screening effect for further improvement on MicroLEDs performance.**

***Index Terms*—MicroLEDs, InGaN/GaN MQWs, V-pits, H_2, Potential Barrier**

I. INTRODUCTION

Because of the AR/VR/MR requirement, Micro-light-emitting diodes (MicroLEDs) has received more and more attention. Due to advantages such as high efficiency, high stability, and long lifetime, InGaN/GaN based self-radiating MicroLEDs displays are considered the next generation display technology [1], [2].

However, the scale production of MicroLEDs still faces enormous challenges, such as low-cost transfer technology, and low efficiency of green MicroLEDs. Due to the large lattice mismatch between GaN and InN, the growth of high-quality and high-indium content green InGaN/GaN multi-quantum wells has always faced many challenges. Besides, the increase of indium content makes the phase separation of indium more serious, leading higher density of dislocations caused by lattice mismatch [3]. The growth of high indium content MQWs requires a higher growth temperature difference between the wells and the barriers, thus Indium atoms may desorb from the surface, leading to the generation of defects and indium segregation near the upper interface of the QWs [4], [5].

For MicroLEDs, even small wavelength fluctuations at the micron level may have a huge impact on yield and increase production costs. What's more, when applied to high-resolution displays, the stability of LEDs is a major requirement under high temperature and various injection current [6], [7]. For the former one, the uniform distribution of indium is crucial, while for the latter one, it is closely related to the crystal quality.

In order to improve the quality and the uniform distribution of indium of MQWs, many researchers have reported the effect of the presence of H_2 during the MQWs growth. Some researchers find that the presence of H_2 during the MQWs growth will create smoother surface and enhanced photoluminescence (PL) [8], [9]. Ren et al. reported that adopting the H_2 pre-flow prior to the InGaN quantum well growth will make the interface smoother and enhance the PL intensity [10]. R. Czernecki, et al. reported that the H_2 flow reduced the indium concentration and thickness of the QWs and increase the thickness of the barriers [11]. However, Wu et al. reported that the MQWs under H_2 treatment has a lower EQE, while the forward and reverse currents will be reduced [12]. Such different results reported may be due to the different H_2 flow rate in the carrier gas or different growth processes of the QWs.

Thermal stability is an important topic in evaluating the performance of MicroLEDs displays. Since a great portion of the applied power on MicroLEDs device lost by heat form. The resulting high junction temperature would cause many problems such as wavelength shifts, photoelectric efficiency, shorter lifetime. As for MicroLEDs, the larger chip density makes this problem even more significant, and seriously affects the display performance.

However, there is few research on the impact and effect of H_2 flow during barrier growth on MicroLEDs and the potential barrier height of the sidewall MQWs. In this work, we investigated H_2 flow during the growth of barrier and discussed the influence mechanism of hydrogen on the growth

Manuscript received 08 February 2024; revised 01 April 2024; accepted 02 April 2024. Date of publication -----; date of current version ----. (Corresponding author: LJ Bao; SP Chang.)

Hsin-Yu Liu and Shoou-Jinn Chang are with the Institute of Microelectronics, Department of Electrical Engineering, National Cheng Kung University, Tainan City, 70101, Taiwan.

Donghao Zhang, Lijun Bao, Zongmin Lin and Chaohsu Lai are with the Department of Electronic Science, Xiamen University, Xiamen, 361005, China (email: baolijun@xmu.edu.cn).

Zhongying Zhang and Chia-En Lee are with the Xiamen San'an Optoelectronic Company Ltd., Xiamen 361005, China.

Sheng-Po Chang is with the Department of Microelectronics Engineering, National Kaohsiung University of Science and Technology, Kaohsiung City, Taiwan (email: changsp@nkust.edu.tw).

This article has been accepted for publication in IEEE Photonics Journal. This is the author's version which has not been fully edited and content may change prior to final publication. Citation information: DOI 10.1109/JPHOT.2024.3386111

of MQWs. We not only focused on the photoluminescence (PL) and electroluminescence (EL) performance, but also the role of screening dislocations by potential barrier height of the sidewall MQWs in V-pits, so-called the V-pits bandgap engineering.

II. Methods

The green MQWs were grown on planar c-plane sapphire substrates by metal–organic chemical vapor deposition (MOCVD) system. The active region is as follows: 9 pairs of $In_{0.25}Ga_{0.75}N$ well (3 nm)/GaN barrier (12 nm) green MQWs were grown after 3 pairs of $In_{0.05}Ga_{0.95}N$ (2 nm)/GaN (45 nm) and 4 periods of $In_{0.1}Ga_{0.9}N$ (2 nm)/GaN (8 nm) and 44.8 nm $In_{0.15}Ga_{0.85}N$ prelayers. The growth process of quantum wells is as follows: after the InGaN layer is deposited, the indium source is cut off to deposit low temperature GaN (LT-GaN) cap layer. After an interruption time, the temperature is raised while hydrogen is introduced into the carrier gas, and the GaN barrier layer was grown in an environment of hydrogen and nitrogen at the same time. To facilitate the comparison, the same structure was designed for the two samples except the H_2 flow during the barrier growth. The H_2 flow was set to be 34.5 sccm for sample 1 and 54.5 sccm for sample 2 respectively, as schematically shown in Fig. 1(a).

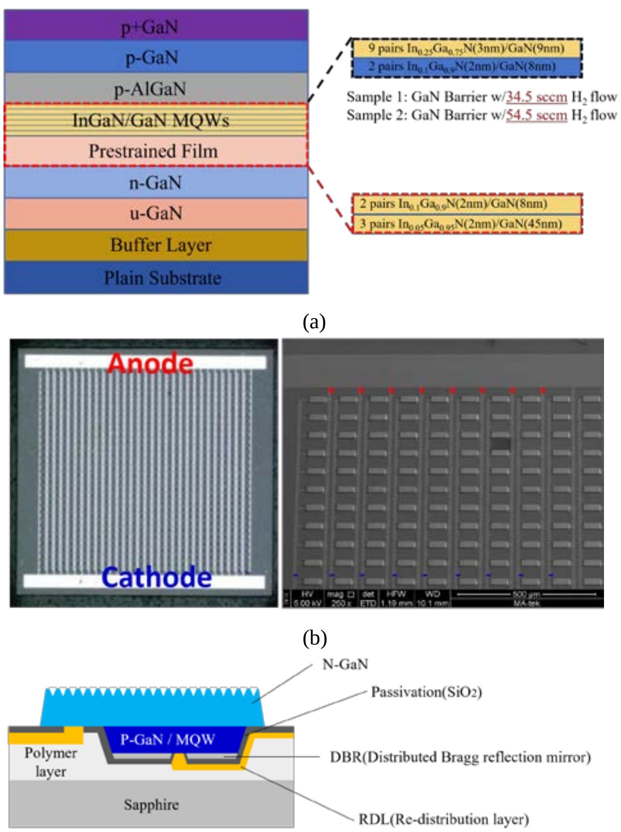

Fig. 1. (a) Schematic illustration of the green LED epitaxy structure and condition for Sample 1 and 2. (b) Single-color MicroLEDs arrays consisting of 900 (30x30) pixels and SEM picture. (c) Schematic illustration of single flip chip type MicroLEDs.

After the epitaxial growth, the two samples are fabricated into the flip chip structure MicroLEDs in size of 34 μm×58 μm with the n-type GaN upwards and roughed. Single-color MicroLEDs arrays consisting of 900 (30 × 30) pixels were fabricated from sample 1 and sample 2 respectively and named as LED 1 and LED 2 by inductively coupled plasma (ICP) etching and UV lithography. Electrodes were deposited on both sides of the pixel mesa. The structure of the MicroLEDs array and the single pixel mesa are shown in Fig 1(b) and Fig 1(c).

Scanning electron microscopy (SEM) images were taken by HITACHI Regulus 8100. The element distributions were taken by a FEI Talos F200X G2 TEM in scanning transmission electron microscope (STEM) mode with energy dispersive X-ray (EDX) system. A 374-nm laser (Coherent OBIS) was used as a PL excitation source, PL signals were collected by spectrometer (Ocean Insight HR4000). Micro-PL mapping pictures were obtained from a hyperspectral imaging spectrometer (Soc710). The temperature dependence of the luminescence spectra was measured from 10 to 300 K in a cryostats (OptistatDry), and samples were excited by a 375-nm laser (MDL-Ⅲ). Spectrometer (Ocean Insight QE Pro) was used to collect PL signals. Cathodoluminescence (CL) experiments were performed using a Delmic SPARC Spectral system and at an acceleration voltage of 5.0 keV and room temperature. The electroluminescence (EL) characteristics were obtained using an integrating sphere (Instrument System) system. Aging testing is conducted on an LED lifespan testing system (WEI MIN LED-800).

III. Results And Discussions

Scanning electron microcopy (SEM) is used to analysis and quantify V-pits size and amount also surface morphology. Sample 1 (H_2 flow 34.5 sccm for barrier growth) and 2 (H_2 flow 54.5 sccm for barrier growth) were prepared with the same condition as samples 1 and 2 but without p-type layers for better observation of V-pits. As shown in Fig. 2(a) and Fig. 2(b), we found many of inverted hexagonal pits distributing on the surface of both samples. The inverted hexagonal pits are so-called V-pits which is a common nanostructure in current commercial InGaN LEDs. The most obvious difference between two samples is the presence of many small V-pits around the large V-pits in sample 1 (H_2 flow 34.5 sccm for barrier growth) as shown by red circle in Fig. 2(a). Their diameters are between 20-80 nm, and some of them can be observed to have a hexagonal structure, similar to the large V-pits construction, and all of them are present around large V-pits. Based on their size, they should be formed in the last few QWs. We speculate that they may be related to fluctuations of indium content and strain accumulation around large V-pits. According to previous research, the energy barrier between V-pits sidewall quantum wells and c-plane quantum wells have a screening effect on the dislocations (TDs) [13]. The screening effect of V-pits is also a consensus by LED community for the high efficiency of InGaN LEDs despite the high dislocation density (~2×10^{8} cm^{-2} on sapphire substrate). This means that

This article has been accepted for publication in IEEE Photonics Journal. This is the author's version which has not been fully edited and content may change prior to final publication. Citation information: DOI 10.1109/JPHOT.2024.3386111

TABLE I
STATISTICAL RESULTS OF V-PITS

Sample	Density of large V-pits(/cm^2)	Density of Small V-pits(/cm^2)	Average diameter of large V-pits(nm)	Average depth of large V-pits(nm)	Average diameter of small V-pits(nm)	Average depth of small V-pits(nm)	Area ratio
sample1	4.41×10^8	6.78×10^7	295	278	43	40	24.91%
sample2	4.44×10^8	0	300	282	none	none	25.94%

TABLE Ⅱ
IQE AND THE FITTED RESULTS WITH RESPECT TO EXPERIMENTAL RESULTS OF TDPL

Sample	Relative IQE(%)	C_1	C_2	E_1 (meV)	E_2 (meV)
sample1	13.8	1.079	53.63	11.76	58.71
sample2	26.9	0.432	19.2	7.24	52.21

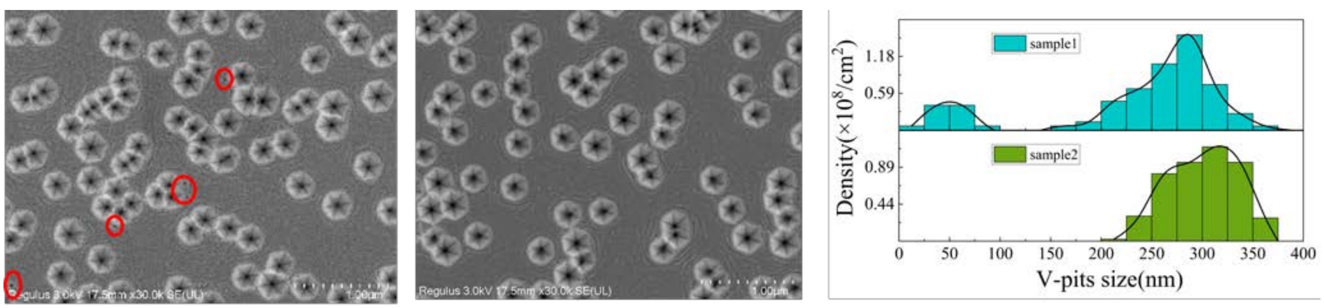

(a) (b) (c)

Fig. 2. SEM images of the surface morphology for (a-b) sample 1-2, and (c) Statistical results of V-shape pits densities and diagonal size.

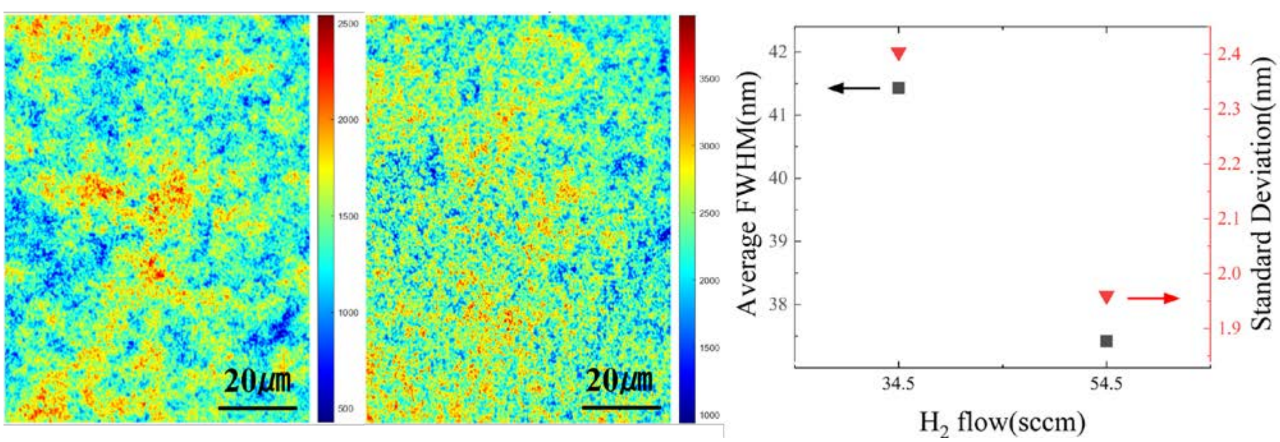

(a) (b) (c)

Fig. 3. Micro-PL peak intensity mapping pictures of sample 1-sample 2(a)-(b). (c) Statistical results of FWHM and FWHM-STD from Micro-PL of sample 1 and sample 2.

it is more difficult for TDs to capture carriers then reduces the radiative recombination rate.

However, the barrier thickness of small pits may be too thin to screen the dislocations (TDs). And some of them appear to have TDs intersecting MQWs without V-pits sidewalls, leading to partially MQWs directly penetrated by TDs. Those lead to a significant decrease in the efficiency of LEDs [14]. In other words, small V-pits represent a higher probability of non-radiative recombination. This will be discussed in detail later.

Fig. 2(c) and Table I show the V-pits density calculated from low magnification TEM images. When the flow rate increases from 34.5 sccm to 54.5 sccm, no small pits were found in our SEM images.

To explain these phenomena, we must first understand how H_2 affects the growth process of quantum wells. There are two main aspects. First, hydrogen will form Ga-H complex with lower adsorption energy with Ga, and increase the diffusion distance of Ga atoms [15], [16], [17]. Second, In atoms might react with hydrogen to form hydride compounds thus lowers the amount of In [18]. When the hydrogen flow rate is small (34.5 sccm), LT-GaN cap layer can protect most of the In atom in the quantum wells. As the hydrogen flow rate increases, the enhanced diffusion of Ga atoms plays a dominant role, which is beneficial in enhancing the 2-dimensional growth and suppresses the formation of new pits especially for small pits that begin to grow in last few quantum wells but has little effect on large V-pits that have already formed before MQWs [19], [20]. Moreover, the hydrogen remove the In-rich clusters from the MQWs, therefor reducing stress accumulation may also played a significant role [12]. According to the Table I, the density and size of large V-pits of two samples are almost the same, but the absence of small V-pits in sample 2 is the major difference and their impact and effect on the MicroLEDs performance will be revealed in below discussion. Micro-PL mapping measurement were used to verify the improvement of luminescence uniformity. As shown in Fig. 3, we can see that as the H_2 flow increases from 34.5 sccm to 54.5 sccm, radiation recombination area gradually increases and the distribution becomes more uniform. This means an improvement in crystal quality and uniformity of MQWs and a reduction in micron-scale indium-rich clusters that generate a large number of defects [21], [22]. Fig. 3(c) shows the full width at half maxima (FWHM) and corresponding standard deviation (STD) calculated from Micro-PL data. As the H_2 flow increases from 34.5 to 54.5 sccm, the average FWHM and corresponding STD decreased from 41.43 nm to 37.42 nm and from 2.40 to 1.96 nm, respectively. For MicroLEDs with a size of only a few tens of micrometers, micron level uniformity of luminescence is crucial for improving MicroLEDs performance.

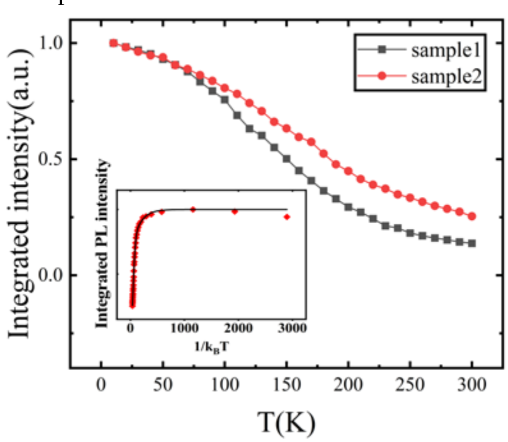

Fig. 4. Temperature dependence of normalized integrated PL intensity for sample 1 and sample 2. The inset picture is Arrhenius plots of the normalized integrated PL intensity for sample 1 and sample 2 over the temperature ranging from 10 K to 300 K.

Temperature dependent photoluminescence (TDPL) was used to verify the reduction of non-radiative recombination rate and measure the relative internal quantum efficiency of the samples. Fig. 4 showed the variation of PL normalized integrated intensity with temperature, we can see that as the temperature increases from 10 K to 300 K, the PL integral intensity of both samples monotonically decreases, which is due to the gradual activation of non-radiative recombination centers [23], [24]. But the decay rate of sample 2 is significantly slower. The PL intensity was fitted by the double-channel Arrhenius equation [27]:

$$I(T)=\left[1+C_1\exp\left(-\frac{E_1}{k_BT}\right)+C_2\exp\left(-\frac{E_2}{k_BT}\right)\right]$$

Where I(T) represent the normalized integrated PL intensity. The parameters C_1 and C_2 are two constants related to the density of non-radiative recombination centers in the samples. E_1 and E_2 are the activation energies related with the non-radiative recombination process [25], [26], [27], [28]. k_B is Boltzmann's constant. Fitting results of two samples were listed in Table Ⅱ. As the hydrogen flow rate increased from 34.5 to 54.5 sccm, C_1 and C_2 decreased from 1.079 to 0.432, and from 53.63 to 19.198 respectively. This further indicated that the strong correlation between H_2 flow during barrier growth and the number of non-radiative recombination centers. The relative internal quantum efficiency (IQE) defined as I_{300K}/I_{10K}, was also significantly increased from 13.8% to 26.9%, as hydrogen flow changed from 34.5 to 54.5 sccm.

As mentioned earlier, due to the energy gap difference between c-plane quantum wells and V-pits sidewall quantum wells, V-pits nanostructure can screen the dislocations (TDs) and thus improve the MicroLEDs efficiency. CL (Cathodoluminescene) was used to investigate the impact of different hydrogen flow and quantify the energy gap difference between V-pits sidewall quantum wells and c-plane quantum wells.

The energy difference between c-plane QW sidewall QW is from two aspects: (1) Compare with c-plane quantum well, sidewall quantum well has thinner well thickness and lower Indium composition, so the sidewall quantum wells have shorter wavelength and higher barrier height. (2) The sidewalls of V-pits are semi-polar planes (R-plane) which means lower piezoelectric field thus emits shorter wavelength and higher barrier height [29]. As shown in Fig. 5, we can observe four CL peaks from the V-pits, P1 and P2 are emission peaks from pre-layers, P4 is the main emission peak of the active region, and P3 at around 500 nm is only observed at the location within V-pits.

In Fig. 5(b), we can see that when the signal acquisition point is away from center of the V-pits on sample 1, P3 gradually weakened and eventually disappeared.

So, we believe that P3 is the emission peak from the sidewall quantum wells, and the difference between the P3 and P4 is considered to be the energy gap between c-plane quantum wells and V-pits sidewall quantum wells, also the potential barrier height that screens dislocations. We

This article has been accepted for publication in IEEE Photonics Journal. This is the author's version which has not been fully edited and content may change prior to final publication. Citation information: DOI 10.1109/JPHOT.2024.3386111

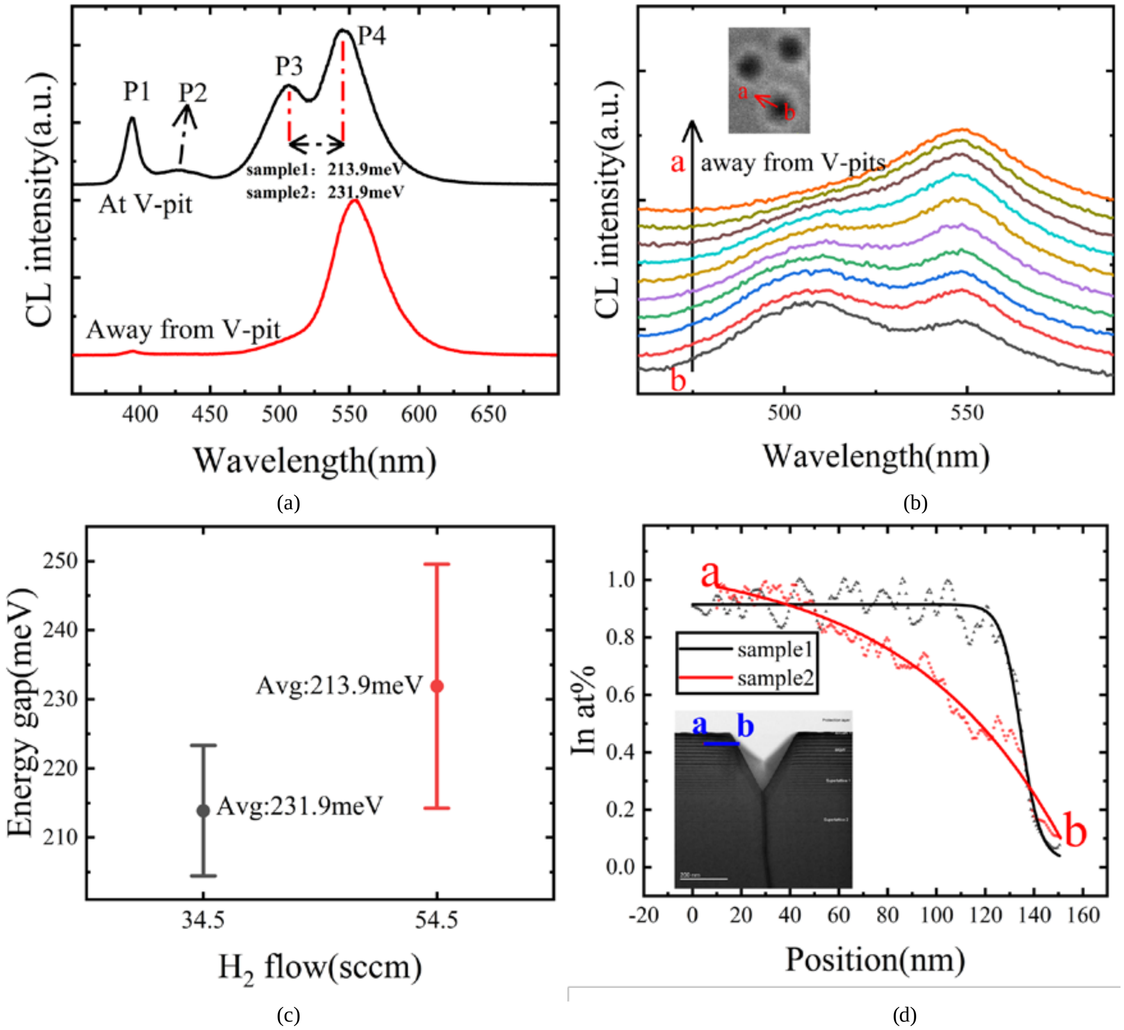

Fig. 5. (a) CL spectrum of samples 1 and sample 2 at the location near the center of V-pits and away from the V-pits. (b) CL spectrum from the location near the center of V-pits to the location away from the V-pits in sample1. (c) Interval graph of energy gap for sample 1 and sample 2. (d) In signals of sample 1 and sample 2 measured by EDX.

calculated the barrier heights measured at dozens of points on two samples, and plotted the result in Fig. 5(c). It's very clear that the average energy gap of sample 1 and sample 2 are 213.9 meV and 231.9 meV respectively. This indicates that the V-pits of sample 2 has higher potential barrier height that suppresses non-radiative recombination functionally. Previously, a series of reports suggested that the height of this barrier mainly depends on the size of V-pits [30], [31], [32]. However, in this experiment, it has been demonstrated through SEM that there is no significant difference in the V-pits size between sample 1 and sample 2. Therefore, this energy gap difference is from indium content difference of the sidewall quantum wells caused by different H_2 flow during barrier growth. In other words, we can modify potential barrier height between c-plane quantum wells and V-pits sidewall quantum wells by controlling the H_2 flow during barrier growth. When H_2 flow through the surface, indium atoms around the core of TDs can be more easily washed out [33]. Moreover, compared to c-plan quantum wells, the thickness of LT-GaN cap layer in V-pits is thinner, therefore, H_2 has a more significant impact

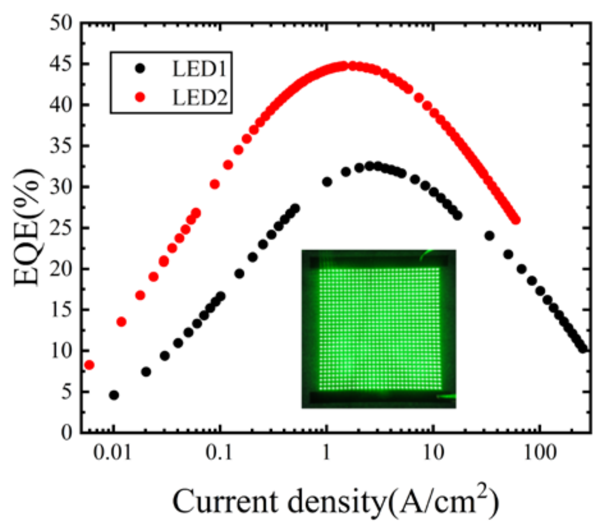

Fig. 6. EQE curves of LED 1 and LED 2.

This article has been accepted for publication in IEEE Photonics Journal. This is the author's version which has not been fully edited and content may change prior to final publication. Citation information: DOI 10.1109/JPHOT.2024.3386111

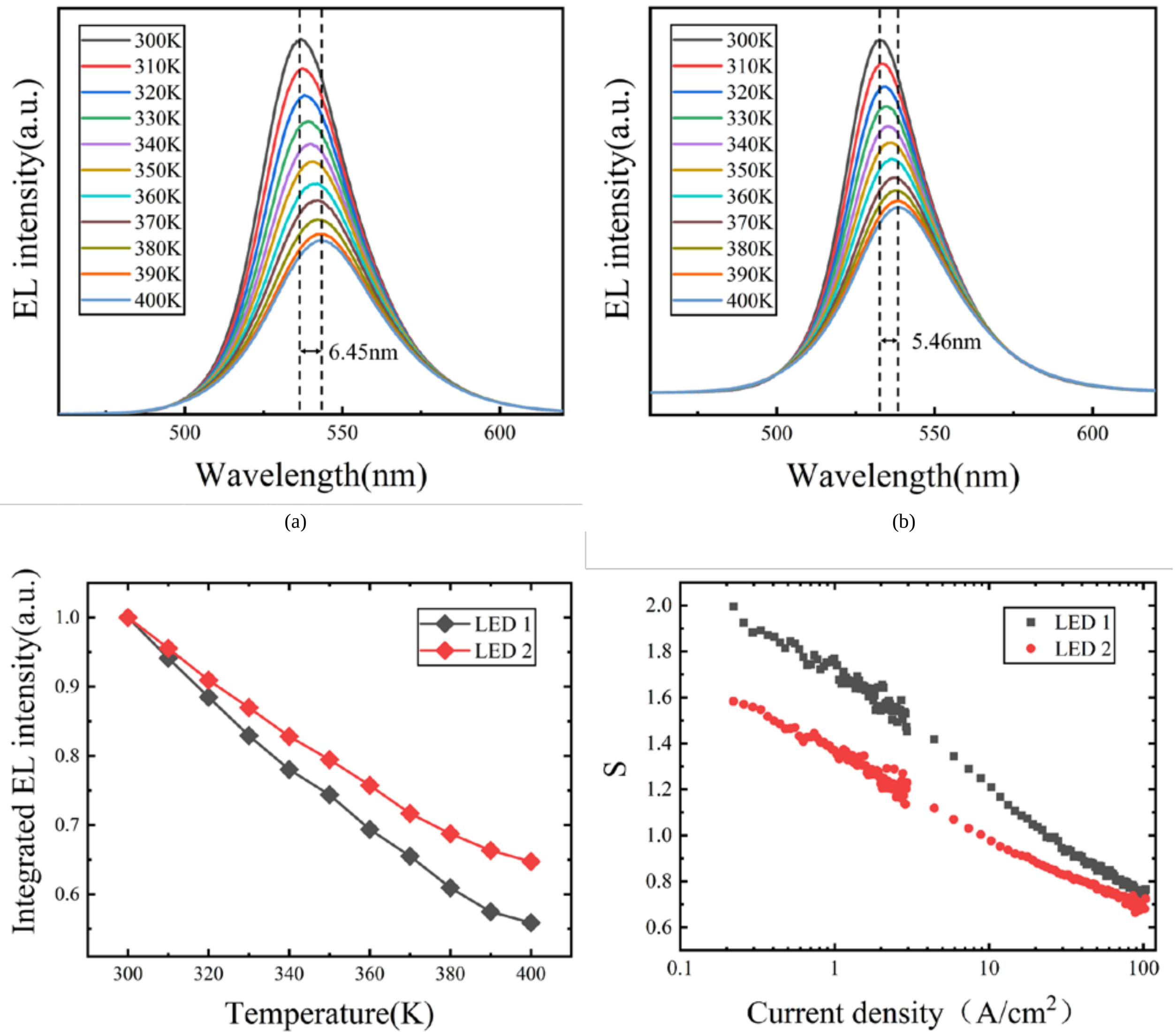

(a) (b) (c) (d)

Fig. 7. (a) EL spectrum of LED 1 from 300 K to 400 K. (b) EL spectrum of LED 2 from 300 K to 400 K. (c) Temperature dependence of normalized integrated EL intensity. (d) S values as a function of current density of LED 1 and LED 2.

on the indium content of sidewall quantum wells. When the hydrogen flow increases from 34.5 sccm to 54.5 sccm, indium content loss in sidewall quantum wells is more severe, and at the same time, the flow of hydrogen has a much smaller impact on the indium content of c-plane quantum wells due to the thicker LT-GaN cap layer on c-plane. This enables the V-pits of sample 2 to have the ability to limit the lateral diffusion of carriers by screening effect and reduce the number of carriers captured by non-radiative recombination by dislocations, and thus improves MicroLEDs internal quantum efficiency.

In order to verify the above assumption, the distribution of Indium atom along the EDX scanning line was conducted and showed in Fig. 5(d). The scanning line was indicated by a blue line in the inset from point a to point b. Near the region close to V-pits, there is a huge difference in the indium distribution between the two samples. When measurement point approach near the V-pits, the indium signal of sample 2 decays faster, which means a sharp drop in indium composition near the sidewall QWs, and the Indium profile difference between the two samples near the V-pits also form a different potential barrier height between c-plane quantum wells and V-pits sidewall quantum wells, which is consistent with the CL results.

To investigate the influence of H_2 on the electrical performance, the EQE of MicroLEDs arrays (900 pixels) was measured by the integral system under different current density. As shown in Fig. 6, the peak EQE of the LED 1 and LED 2 is 32.5% and 44.8%, respectively. And the corresponding injection current density is 2.54 and 1.76 A/cm^2, respectively. EQE of LED 2 is higher than LED within all measurement range, especially in low current density about 1A/cm^2.The inset shows uniform light distribution picture of MicroLEDs arrays (900 pixels) under current density of 2.5 A/cm^2. This indicates that LED 2 with a H_2 flow of 54.5 sccm during the barrier growth is more suitable for the need of low power consumption in high-resolution MicroLEDs displays [34].

As introduction mentioned, the temperature stability and behavior are important for MicroLEDs display application. Temperature dependence of the EL was conducted at a forward current of 3.9 A/cm^2 to investigate the temperature characteristics of the two samples. As shown in Fig. 7(a) and Fig. 7(b), when the temperature increased from 300 K to 400 K, LED 1 had a red-shift of 6.45 nm, while LED 2 had a red-shift of 5.46 nm, which was caused by shrinking of the InGaN band-gap. However, the red-shift of LED 1 is large than that of LED 2. This is due to the higher density of Shockley-Read-Hall recombination centers in LED 1, resulting more heat accumulation during operation.

On the other hand, the EL intensity gradually decreases as the temperature increases. It can be clearly seen in Fig. 7(c) that LED 1 has a higher decay ratio of EL intensity. When the temperature increases from 300 K to 360 K, the brightness of LED 1 and LED 2 decreases to 69.24% and 76.65%, respectively. As the temperature further increases to 400 K, the brightness decreases to 55.74% and 64.61%, respectively, which indicate the smaller temperature dependence of LED 2. This is because there are less SRH recombination centers in the active region of LED 2. The SRH recombination became more effective and led to less carriers for radiative recombination in the active region when temperature increased [27]. It's clear that LED 2 has better thermal stability in wavelength and EL intensity when operate at high temperature.

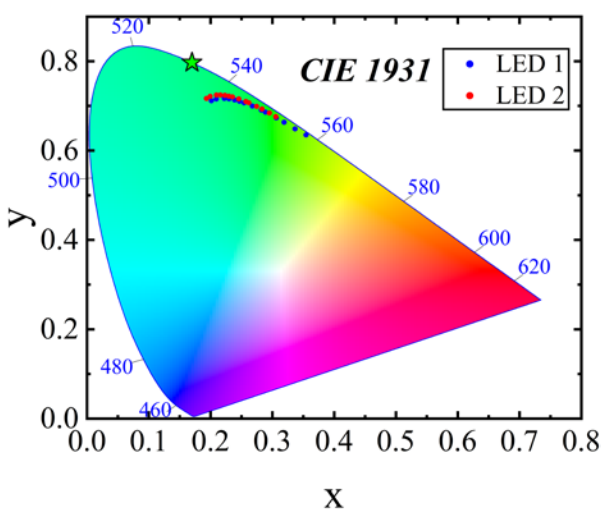

Fig. 8. CIE1931 diagram of two samples at the current density from 2 to 100 A/cm^2.

S values can be used to investigate the carrier recombination mechanism of the InGaN based LED. If S value equals to 2, it means SRH recombination dominates. If S equals to 1, it means radiative recombination dominates. When S value is less than 1, it indicates carrier leakage. Fig. 7(d) shows the S values calculated by L-I curves of LED 1 and LED 2. When the current density is between 0.2 and 1 A/cm^2, the S values of both samples are close to 2, indicated that SRH recombination dominates at such a small current intensity, and the S value of LED 2 is significantly closer to 2. This means that under low current density, the defect related SRH recombination rate in LED 2 is smaller, further indicating that LED 2 has a smaller defect density and better crystal quality [35].

To estimate the influence of current density in the color space, CIE 1931 positions of LED 1 and LED 2 at 2 to 100 A/cm^2 are shown in Fig. 8. We can see that LED 2 exhibits more stable coordinates and smaller shift when operation current density is from 2 to 100 A/cm^2. This phenomenon is more pronounced at low current densities region. At high current density, the color coordinates of LED 2 are closer to the defined green color in Rec. 2020 (0.17, 0.797) compared to LED 1. These indicate that LED 2 has better color stability and higher color saturation for MicroLEDs display application.

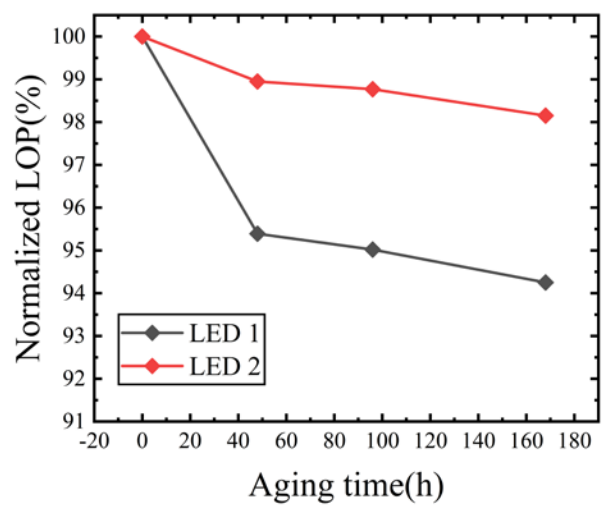

(a)

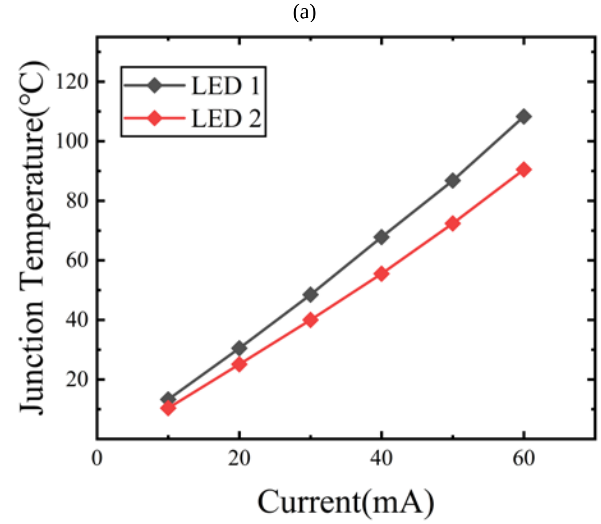

(b)

Fig. 9. (a) Lop (Brightness) of LED 1 and LED 2 after aging time. (b) Junction temperature at different currents.

After a long period of operation, the recombination mechanism of LEDs will change, leading to a decay of light output power. To confirm whether there is a difference in the lifetime of the two MicroLEDs, a high operation current density of 233 A/cm^2 was applied to each MicroLEDs at 360 K ambient temperature for aging test. The test results are shown in Fig. 9(a). In the first 48 hours, there was a significant decay in light output power, followed by a slower decay process. We can clearly see that the brightness decay of LED 1 is much severe than that of LED 2, indicating that LED 2 has a longer lifetime and better reliability. This difference may be caused by the lower density of non-radiative recombination centers in LED 2. It is reported that the degradation of LED is related to the increase in non-radiative recombination [36], [37]. Fig. 9(b) shows the junction temperature measured under different currents. It can be seen that the junction temperature of LED 2 is always lower than that of LED 1, and this difference gradually larger as the current increases. We believe that this is caused by a reduction in non-radiative recombination that generate heat. The longer lifetime and lower junction temperature proved that LED 2 is more suitable for display field applications.

III. CONCLUSION

In conclusion, we analyzed the characteristics of two samples with different hydrogen flow ranging from 34.5 to 54.5 sccm during barrier growth. A detailed discussion was conducted to verify the influence mechanism of H_2 flow of MQWs and the impact on the MicroLEDs performance, and it was found that the improvement in performance mainly comes from the reduction of non-radiative recombination centers and higher energy gap of V-pits between c-plane quantum wells and V-pits sidewall quantum wells. These two factors cause a significant decrease in non-radiative recombination rate. The sample with a hydrogen flow of 54.5 sccm has advantages in radiation efficiency, brightness uniformity, thermal endurance, CIE behavior and excellent lifetime. This study demonstrates that the performances of Micro-LED can be effectively improved by modification of hydrogen flow during barrier growth and V-Pits bandgap engineering. We provide a new concept that not only the V-pits size but also modification of H_2 flow during barrier growth that affects screening effect of V-pits. Our results offer a guideline for future MicroLEDs development.

REFERENCES

[1] T. Wu et al., "Mini-LED and Micro-LED: Promising Candidates for the Next Generation Display Technology," *Appl. Sci*., vol. 8, no. 9, p. 1557, Sep. 2018, doi: 10.3390/app8091557.

[2] M. S. Wong, S. Nakamura, and S. P. DenBaars, "Review—Progress in High Performance III-Nitride Micro-Light-Emitting Diodes," *ECS J. Solid State Sci. Technol*., vol. 9, no. 1, p. 015012, 2020, doi: 10.1149/2.0302001JSS.

[3] M. Auf Der Maur, A. Pecchia, G. Penazzi, W. Rodrigues, and A. Di Carlo, "Efficiency Drop in Green InGaN / GaN Light Emitting Diodes: The Role of Random Alloy Fluctuations," *Phys. Rev. Lett*., vol. 116, no. 2, p. 027401, Jan. 2016, doi: 10.1103/PhysRevLett.116.027401.

[4] J. Yang et al., "Photovoltaic response of InGaN/GaN multi-quantum well solar cells enhanced by inserting thin GaN cap layers," *J. Alloys Compd*., vol.635, pp.82-86, Jun.2015, doi: 10.1016/j.jallcom.2015.02. 052.

[5] C. Zheng, L. Wang, C. Mo, W. Fang, and F. Jiang, "Effect of Same-Temperature GaN Cap Layer on the InGaN/GaN Multiquantum Well of Green Light-Emitting Diode on Silicon Substrate," *Sci. World J.*, vol. 2013, pp. 1–4, 2013, doi: 10.1155/2013/538297.

[6] J.-C. Lee, Y.-F. Wu, Y.-P. Wang, and T.-E. Nee, "Temperature and current dependences of electroluminescence from InGaN/GaN multiple quantum wells," *J. Cryst. Growth*, vol. 310, no. 23, pp. 5143–5146, Nov. 2008, doi: 10.1016/j.jcrysgro.2008.06.077.

[7] S. Ishimoto et al., "Enhanced Device Performance of GaInN-Based Green Light-Emitting Diode with Sputtered AlN Buffer Layer," *Appl. Sci*., vol. 9, no. 4, p. 788, Feb. 2019, doi: 10.3390/app9040788.

[8] X. Ren, J. R. Riley, D. D. Koleske, and L. J. Lauhon, "Correlated high-resolution x-ray diffraction, photoluminescence, and atom probe tomography analysis of continuous and discontinuous InxGa1−xN quantum wells," *Appl. Phys. Lett*., vol. 107, no. 2, p. 022107, Jul. 2015, doi: 10.1063/1.4926808.

[9] F. Massabuau, M. Kappers, C. Humphreys, and R. Oliver, "Mechanisms preventing trench defect formation in InGaN/GaN quantum well structures using hydrogen during GaN barrier growth," *Phys. Status Solidi B*, vol. 254, no. 8, p. 1600666, Aug. 2017, doi: 10.1002/pssb.201600666.

[10] P. Ren, N. Zhang, B. Xue, Z. Liu, J. Wang, and J. Li, "A novel usage of hydrogen treatment to improve the indium incorporation and internal quantum efficiency of green InGaN/GaN multiple quantum wells simultaneously," *J. Phys. Appl. Phys*., vol. 49, no. 17, p. 175101, May 2016, doi: 10.1088/0022-3727/49/17/175101.

[11] R. Czernecki et al., "Effect of hydrogen during growth of quantum barriers on the properties of InGaN quantum wells," *J. Cryst. Growth*, vol. 414, pp. 38–41, Mar. 2015, doi: 10.1016/j.jcrysgro.2014.09.037.

[12] Y. Wang et al., "Effect of Hydrogen Treatment on Photoluminescence and Morphology of InGaN Multiple Quantum Wells," *Nanomaterials*, vol. 12, no. 18, p. 3114, Sep. 2022, doi: 10.3390/nano12183114.

[13] A. Hangleiter et al., "Suppression of Nonradiative Recombination by V-Shaped Pits in GaInN / GaN Quantum Wells Produces a Large Increase in the Light Emission Efficiency," *Phys. Rev. Lett*., vol. 95, no. 12, p. 127402, Sep. 2005, doi: 10.1103/PhysRevLett.95.127402.

[14] W. Qi et al., "Effects of thickness ratio of InGaN to GaN in superlattice strain relief layer on the optoelectrical properties of InGaN-based green LEDs grown on Si substrates," *J. Appl. Phys*., vol. 122, no. 8, p. 084504, Aug. 2017, doi: 10.1063/1.5000134.

[15] Q. Wu et al., "Effects of Hydrogen Treatment in Barrier on the Electroluminescence of Green InGaN/GaN Single-Quantum-Well Light-Emitting Diodes with V-Shaped Pits Grown on Si Substrates," *Chin. Phys.* Lett., vol. 35, no. 9, p. 098501, Sep. 2018, doi: 10.1088/0256-307X/35/9/098501.

[16] X. H. Wu et al., "Structural origin of V-defects and correlation with localized excitonic centers in InGaN/GaN multiple quantum wells," *Appl. Phys. Lett*., vol. 72, no. 6, pp. 692–694, Feb. 1998, doi: 10.1063/1.120844.

[17] R. Czernecki et al., "Influence of hydrogen and TMIn on indium incorporation in MOVPE growth of InGaN layers," *J. Cryst. Growth*, vol.402, pp. 330–336, Sep. 2014, doi: 10.1016/j.jcrysgro.2014.05.027.

[18] Y. Morishita, Y. Nomura, S. Goto, and Y. Katayama, "Effect of hydrogen on the surface-diffusion length of Ga adatoms during molecular-beam epitaxy," *Appl. Phys. Lett*., vol. 67, no. 17, pp. 2500–2502, Oct. 1995, doi: 10.1063/1.114438.

[19] A. Sohmer et al., "GaInN/GaN-Heterostructures and Quantum Wells Grown by Metalorganic Vapor-Phase Epitaxy," *MRS Internet J. Nitride Semicond. Re*s., vol. 2, p.e14,1997, doi: 10.1557/S1092578300001 40X.

[20] X. Zhou et al., "Surface Morphology Evolution Mechanisms of InGaN/GaN Multiple Quantum Wells with Mixture N_2/H_2-Grown GaN Barrier," *Nanoscale Res. Lett*., vol. 12, no. 1, p. 354, Dec. 2017, doi: 10.1186/s11671-017-2115-8.

[21] I.-H. Kim, H.-S. Park, Y.-J. Park, and T. Kim, "Formation of V-shaped pits in InGaN/GaN multiquantum wells and bulk InGaN films," *Appl. Phys. Lett*., vol. 73, no. 12, pp. 1634–1636, Sep. 1998, doi: 10.1063/1.122 229.

[22] Y. Hou, F. Liang, D. Zhao, P. Chen, J. Yang, and Z. Liu, "Role of hydrogen treatment during the material growth in improving the photoluminescence properties of InGaN/GaN multiple quantum wells," *J. Alloys Compd*., vol. 874, p. 159851, Sep. 2021, doi: 10.1016/j.jallcom.2021.159851.

[23] X. Tao et al., "Performance enhancement of yellow InGaN-based multiple-quantum-well light-emitting diodes grown on Si substrates by optimizing the InGaN/GaN superlattice interlayer," *Opt. Mater. Express*,vol. 8, no. 5, p. 1221, May 2018, doi: 10.1364/OME.8.001221.

[24] H. Wang et al., "Influence of excitation power and temperature on photoluminescence in InGaN/GaN multiple quantum wells," O*pt. Express*,vol. 20, no. 4, p. 3932, Feb. 2012, doi: 10.1364/OE.20.003932.

[25] Y. Fang et al., "Investigation of temperature-dependent photoluminescence in multi-quantum wells," *Sci. Rep*., vol. 5, no. 1, p. 12718, Jul. 2015, doi: 10.1038/srep12718.

[26]J. S. Hwang et al., “Comparative investigation of InGaN quantum well laser diode structures grown on freestanding GaN and sapphire substrates,” J. *Appl. Phys*., vol. 102, no. 1, p. 013508, Jul. 2007, doi: 10.1063/1.2749281.

[27]Y. Zhu et al., “Origin of huge photoluminescence efficiency improvement in InGaN/GaN multiple quantum wells with low-temperature GaN cap layer grown in N_2 /H_2 mixture gas,” *Appl. Phys. Express*, vol. 10, no. 6, p. 061004, Jun. 2017, doi: 10.7567/APEX.10.06 1004.

[28]T. Lu et al., “Temperature-dependent photoluminescence in light-emitting diodes,” *Sci. Rep*., vol. 4, no. 1, p. 6131, Aug. 2014, doi: 10.1038/srep06131.

[29]L. Liu et al., “Influence of indium composition in the prestrained InGaN interlayer on the strain relaxation of InGaN/GaN multiple quantum wells in laser diode structures,” *J. Appl. Phys*., vol. 109, no. 7, p. 073106, Apr. 2011, doi: 10.1063/1.3569848.

[30]J.-D. Gao et al., “Detailed surface analysis of V-defects in GaN films on patterned silicon(111) substrates by metal–organic chemical vapour deposition,” *J. Appl. Crystallogr*., vol. 52, no. 3, pp. 637–642, Jun. 2019, doi: 10.1107/S1600576719005521.

[31]N. Okada, H. Kashihara, K. Sugimoto, Y. Yamada, and K. Tadatomo, “Controlling potential barrier height by changing V-shaped pit size and the effect on optical and electrical properties for InGaN/GaN based light-emitting diodes,” *J. Appl. Phys*., vol. 117, no. 2, p. 025708, Jan. 2015, doi: 10.1063/1.4905914.

[32]S. Zhou and X. Liu, “Effect of V-pits embedded InGaN/GaN superlattices on optical and electrical properties of GaN-based green light-emitting diodes,” *Phys. Status Solidi A*, vol. 214, no. 5, p. 1600782, May 2017, doi: 10.1002/pssa.201600782.

[33]S. Zhou et al., “The effect of nanometre-scale V-pits on electronic and optical properties and efficiency droop of GaN-based green light-emitting diodes,” *Sci. Rep*., vol. 8, no. 1, p. 11053, Jul. 2018, doi: 10.1038/s41598-018-29440-4.

[34]M. Shiojiri, C. C. Chuo, J. T. Hsu, J. R. Yang, and H. Saijo, “Structure and formation mechanism of V defects in multiple InGaN⁄GaN quantum well layers,” *J. Appl. Phys*., vol. 99, no. 7, p. 073505, Apr. 2006, doi: 10.1063/1.2180532.

[35]F. Xu et al., “Optimized InGaN/GaN Quantum Structure for High-Efficiency Micro-LEDs Displays With Low Current Injection,” *IEEE Trans. Electron Devices*, vol. 70, no. 8, pp. 4257–4263, Aug. 2023, doi: 10.1109/TED.2023.3283942.

[36]K.-S. Kim, D.-P. Han, H.-S. Kim, and J.-I. Shim, “Analysis of dominant carrier recombination mechanisms depending on injection current in InGaN green light emitting diodes,” *Appl. Phys. Lett*., vol. 104, no. 9, p. 091110, Mar. 2014, doi: 10.1063/1.4867647.

[37]T.-R. Zhang et al., “Aging mechanism of GaN-based yellow LEDs with V-pits*,” *Chin. Phys. B*, vol. 28, no. 6, p. 067305, Jun. 2019, doi: 10.1088/1674-1056/28/6/067305.

[38]M. La Grassa et al., “Ageing of InGaN-based LEDs: Effects on internal quantum efficiency and role of defects,” *Microelectron. Reliab*., vol. 55, no.9–10, pp.1775–1778, Aug.2015, doi: 10.1016/j.microrel.2015. 06.103.